European Polymer Journal 196 (2023) 112273

Contents lists available at ScienceDirect

European Polymer Journal

journal homepage: www.elsevier.com/locate/europolj

Synthesis and characterization of dendronized side chain liquid crystalline Poly(2-oxazoline)s towards biomimetic ion channels

Jordi Guardià [a], Marta Giamberini [b], José Antonio Reina [a], Xavier Montané [a,*]

[a] Universitat Rovira i Virgili, Department of Analytical Chemistry and Organic Chemistry, C/Marcel·lí Domingo 1, 43007 Tarragona, Spain
[b] Universitat Rovira i Virgili, Department of Chemical Engineering, Av. Països Catalans 26, 43007 Tarragona, Spain

ARTICLE INFO

Keywords:
Poly(2-oxazoline)s
Cationic ring-opening polymerization
Side chain liquid crystalline polymers
Biomimetic
Columnar mesophase
Supramolecular structures

ABSTRACT

The polymerization of dendronized monomers is an attractive option to synthesize liquid crystalline columnar polymers with side chain dendrons. Following this approach, we report for the first time in the present study the synthesis of a family of side chain liquid crystalline (SCLC) poly(2-oxazoline)s, poly(2-(3,4,5-tris(4-dodecyloxybenzyloxy)phenyl)-2-oxazoline) (PTOx) from its oxazoline monomer precursor, 2-(3,4,5-tris(4-dodecyloxybenzyloxy)phenyl)-4,5-dihydro-1,3-oxazole) (TAPOx), by cationic ring-opening polymerization (CROP). The optimisation of the reaction parameters (temperature, type of initiator, terminating agent, solvent and monomer concentration), combined with the nature of the CROP allowed us to obtain high molecular weight SCLC poly(2-oxazoline)s. NMR investigations were consistent with the targeted molecular weights of the synthesized PTOx and the living nature of TAPOx polymerization. Regarding the mesomorphic characterization, all synthesized acyl-substituted poly(ethyleneimine)s exhibited liquid crystalline mesophases in a broad temperature range. XRD studies demonstrated that these dendronized poly(2-oxazoline)s self-assemble into columnar structures. Mesomorphic and thermal properties suggest that these family of poly(2-oxazoline)s could be excellent candidates to build up membranes for proton transport applications.

1. Introduction

Nowadays, most of polymer proton exchange membranes are based on perfluorosulfonic acid ionomer (PFSI). Among them, Nafion® (a registered trademark of DuPont Co.) based membranes are the most used due to their excellent electrochemical stabilities, as well as proton conductivities. However, Nafion® presents some drawbacks: (I) an elevated cost due to its complicated manufacturing process, (II) insufficient resistance to methanol crossover and (III) poor mechanical and chemical stability at high temperatures [1]. In order to overcome these drawbacks, other types of polymers have been investigated in recent years [2,3].

Side chain liquid crystalline polymers (SCLCPs) have raised a great interest due to their self-assembly ability, which provides them unique mechanical, optical and electrical properties. For this reason, SCLCPs have been used in a wide range of applications such as optical devices [4], membrane separation [5,6] and solid polymer electrolytes [7,8], among others.

In the second half of 1960′s, four independent research groups reported the synthesis of different poly(2-oxazoline)s [9–12]. These groups proposed their synthesis by thermally induced cationic ring-opening polymerization (CROP). Poly(2-alkyl/aryl-2-oxazoline)s (PAOx) are a family of polymers that has raised a great interest, since their properties can be easily modified by end-group modification, initiator modification, as well as by modifying the pendant group of the 2-substituted-2-oxazoline monomer [13].

In recent years, PAOx received on-going research interest in the biomedical field, due to their biocompatibility [14–17], low toxicity, protein adsorption and stealth behaviour; all these features are similar to those of poly(ethylene glycol) (PEG) (also known as poly(ethylene oxide) (PEO)). Actually, PAOx are an emerging class of polymers who could substitute, even outperform PEG, regarding its increased antifouling behaviour [18–20]. Sedlacek and co-workers developed a method for the synthesis of superhydrophilic PAOx, obtaining poly(2-methoxymethyl-2-oxazoline) which is the most hydrophilic PAOx reported to date [19]. Furthermore, Percec and co-workers reported the first liquid crystalline poly(2-oxazoline) synthesized by CROP, which contains a side chain mesogenic group, describing the synthesis of a SCLC poly(2-oxazoline) [21,22].

During the last two decades, our group has mainly focused on the

* Corresponding author.
E-mail address: xavier.montane@urv.cat (X. Montané).

https://doi.org/10.1016/j.eurpolymj.2023.112273
Received 18 April 2023; Received in revised form 26 June 2023; Accepted 28 June 2023
Available online 29 June 2023

synthesis of dendronized liquid crystalline polyethers [23,24] and polyamines [25–27] by grafting a tapered group on these polymers as a post polymerization procedure. This tapered group induces the self-assembly of the polymer into columnar structures, which contain an inner channel formed by the polyether or the polyamine main chain, respectively, that work as an ion transport channel. However, in the case of the polyamines synthetized by us, they exhibit a strong tendency to crystallize, which results in poor mechanical properties and brittleness. This can be due either to the low molecular weight of the polyamine and the presence of free hydroxyl groups contained in the pendant group of the polymer main chain. However, supported membranes based on these SCLC polyamines showed a remarkable proton transport [26,27].

Hence, in this article we describe the synthesis and characterization of novel liquid crystalline dendronized poly(2-oxazoline)s, poly(2-(3,4,5-tris(4-dodecyloxybenzyloxy)phenyl)-2-oxazoline)s (PTOx). PTOx has been successfully synthetized by "living" CROP, using methyl trifluoromethanesulfonate (MeOTf) as an initiator and morpholine as a terminating agent, after testing several initiators and terminating agents. Besides, the "living" character of this cationic ring-opening polymerization allowed us to precisely control the final molecular weight of the synthesized poly(2-oxazoline)s, obtaining a family of acyl-substituted poly(ethyleneimine)s in a range between 20 and 60 kDa. Due to the presence of nitrogen in the polymer backbone, PTOx can be a promising candidate material to prepare membranes able to transport different ions. This new type of polymer should present improved mechanical properties, in comparison with previously reported polyamines, due to the absence of free hydroxyl groups, and higher and controlled molecular weight.

2. Experimental section

2.1. Materials

Methyl trifluoromethanesulfonate (MeOTf, ≥98 %), 1-dodecylamine (98 %), piperidine (99 %), anhydrous benzotrifluoride (BTF, ≥99 %), methyl *p*-toluenesulfonate (MeOTs, 98 %), 2-(isopropylamino)ethanol (70 %) and chlorobenzene were supplied by Sigma Aldrich. 2,3-dichloro-5,6-dicyano-1,4-benzoquinone (DDQ, 98 %) and morpholine (99 %) were purchased from Alfa Aesar. Triphenylphosphine (PPh_3, 99 %) and benzyl bromide (98 %) were supplied by Across Organics, while dichloromethane (DCM), toluene and *o*-dichlorobenzene (*o*-DCB) were purchased from Scharlab. Furthermore, toluene, chlorobenzene, *o*-DCB, morpholine and 2-(isopropylamino)ethanol were dried prior to use according to literature [28].

2.2. Synthesis of 2-(3,4,5-tris(4-dodecyloxybenzyloxy)phenyl)-4,5-dihydro-1,3-oxazole) (TAPOx)

2-(3,4,5-tris(4-dodecyloxybenzyloxy)phenyl)-4,5-dihydro-1,3-oxazole) (TAPOx) monomer was synthetized following a slight modification of a reported procedure that involved easier workup and higher yield [29]:

In a previously dried Schlenk tube, 2.61 g of PPh_3 (9.95 mmol) and 2.30 g of DDQ (10.14 mmol) were dissolved in 80 mL of dry DCM under argon atmosphere. Then, the mixture was stirred for 3 min at room temperature (RT = 25 ± 5 °C). At once, 7.04 g of *N*-(2-hydroxyethyl)-3,4,5-tris(4-dodecyloxybenzyloxy)benzamide (TAPAm) (6.80 mmol) was then added. The reaction was monitored by TLC using n-hexane/ethyl acetate (1:2) as mixture of eluents. After 20 min, when a complete conversion of TAPAm was reached, the crude mixture was washed with an aqueous NaOH solution (5 wt%, 80 mL). After that, the separated water layer was back-extracted with DCM (50 mL × 4). The two organic layers were combined and washed together with brine solution, dried over anhydrous $MgSO_4$ and the solvent was vacuum evaporated. At this point, the brown solid was purified by recrystallization twice with ethanol. Finally, the product was dried under vacuum at 40 °C overnight to yield 6.16 g of a white solid (89 %).

^{1}H NMR [$CDCl_3$, δ, ppm]: 7.25 (d, 4H, -O-**Ar-H**-CH_2-O-Ar-C = N- from 2 and 6 positions of the lateral benzylic units), 7.21 (s, 2H, **Ar-H**-C = N-), 7.17 (d, 2H, -O-**Ar-H**-CH_2-O-Ar-C = N- from 2 and 6 positions of the central benzylic unit), 6.83 (d, 4H, -O-**Ar-H**-CH_2-O-Ar-C = N- from 3 and 5 positions of the lateral benzylic units), 6.67 (d, 2H, -O-**Ar-H**-CH_2-O-Ar-C = N- from 3 and 5 positions of the central benzylic unit), 4.96 (s, 4H, –**CH_2**-O-Ar-C = N- in lateral benzylic units), 4.91 (s, 2H, –**CH_2**-O-Ar-C = N- in central benzylic unit), 4.34 (t, 2H, -C = N-CH_2-**CH_2**-O-), 3.97 (t, 2H, -C = N-**CH_2**-CH_2-O-), 3.89 (t, 4H, -Ar-O-**CH_2**-$(CH_2)_{10}$-CH_3 in lateral benzylic units), 3.84 (t, 2H, -Ar-O-**CH_2**-$(CH_2)_{10}$-CH_3 in central benzylic unit), 1.70 (m, 6H, -Ar-O-CH_2-**CH_2**-$(CH_2)_9$-CH_3), 1.38 (m, 6H, -Ar-O-CH_2-CH_2-**CH_2**-$(CH_2)_8$-CH_3), 1.20 (m, 48H, -Ar-O-CH_2-CH_2-CH_2-**$(CH_2)_8$**-CH_3), 0.81 (t, 9H, -Ar-O-CH_2-$(CH_2)_{10}$-**CH_3**).

^{13}C NMR [$CDCl_3$, δ, ppm]: 164.7 (-**C** = N-), 159.1 (**ArC**-O-$(CH_2)_{11}$-CH_3 in lateral and central benzylic units), 152.9 (**ArC** meta to -C = N-), 141.2 (**ArC** para to -C = N-), 130.4 (**ArC** meta to -O-$(CH_2)_{11}$-CH_3 in central benzylic unit), 129.7 (**ArC**-CH_2-O-Ar-C = N- in central benzylic unit), 129.4 (**ArC** meta to -O-$(CH_2)_{11}$-CH_3 in lateral benzylic units), 128.9 (**ArC**-CH_2-O-Ar-C = N- in lateral benzylic units), 122.9 (**ArC**-C = N-), 114.6 (**ArC** ortho to -O-$(CH_2)_{11}$-CH_3 in lateral benzylic units), 114.2 (**ArC** ortho to -O-$(CH_2)_{11}$-CH_3 in central benzylic unit), 107.9 (**ArC** ortho to -C = N-), 74.8 (–**CH_2**-O-Ar-C = N- in central benzylic unit) 71.2 (–**CH_2**-O-Ar-C = N- in lateral benzylic units), 68.2 (–**CH_2**-$(CH_2)_{10}$-CH_3 in central and lateral benzylic units), 67.9 (-C = N-CH_2-**CH_2**-O-), 55.0 (-C = N-**CH_2**-CH_2-O-), 32.1 (–**CH_2**-CH_2-CH_3), 29.8–29.5 (-**$(CH_2)_6$**-CH_2-CH_3 and –**CH_2**-$(CH_2)_9$-CH_3), 26.2 (–**CH_2**-$(CH_2)_8$-CH_3), 22.8 (–**CH_2**-CH_3), 14.3 (–**CH_3**).

FT-IR (cm^{-1}): 2950 (ν (C–H) in –CH_3 (asymmetric)); 2917 – 2848 (ν (C–H) in –CH_3 (symmetric) and –CH_2- (asymmetric and symmetric)); 1643 (ν (C = N)); 1588 (ν (C = C–C aromatic)); 1514 (ν (C = C–C aromatic)); 1245 (ν (=C-O-C) asymmetric); 818 (δ (C–H) *p*-disubstitution).

2.3. Synthesis of poly(2-(3,4,5-tris(4-dodecyloxybenzyloxy)phenyl)2-oxazoline)s (PTOx) (Scheme 1)

From all the attempts, the best conditions for the polymerization of TAPOx monomer to achieve "living" behaviour are summarized as follows:

A previously flame dried Schlenk tube was filled with TAPOx (0.5 g, 0.5 mmol) and kept under vacuum for 30 min. After that, the tube was immersed in a previously heated oil bath at 105 °C. When TAPOx was melted, the appropriate amount of dry chlorobenzene was added to reach 1.0 M concentration inside the Schlenk tube (considering the amount of chlorobenzene that is already added with the initiator). Then, the initiator (MeOTf) was added via syringe according to the desired degree of polymerization (DP) from a freshly prepared solution of the initiator in dry chlorobenzene ([MeOTf] = 0.135 M). The mixture was stirred until ^{1}H NMR spectrum indicated almost complete conversion of the monomer (≥93 %). Then, a large excess of morpholine (200 μL) was added to the reaction mixture, acting as a terminating agent. After 30 min, the crude mixture was precipitated twice in a cold KOH solution (0.1 M). Finally, the product was dried under vacuum at 50 °C until constant weight to obtain a beige solid. Monomer conversion was estimated by ^{1}H NMR, comparing the integration of the signal attributed to the methylene contiguous to the nitrogen atom of the monomer oxazoline ring (3.97 ppm) with the integration of the signal attributed to the methyl groups of the long aliphatic chain of the tapered side dendron. The number of each member of the family indicates the expected quantity of repeating units it contains. NMR and FT-IR data of PTOx40 is shown below:

^{1}H NMR [Fig. 1, $CDCl_3$, δ, ppm]: 7.34 – 6.25 (Ar), 5.23 – 4.20 (i, i'), 4.03 – 3.42 (f, g, s, y, 1), 2.35 (x) 1.62 (2), 1.19 (3–11), 0.81 (12).

^{13}C NMR [Fig. 3, $CDCl_3$, δ, ppm]: 171.8 (q), 158.9 (VIII), 152.9 (III), 138.9 (IV), 129.9 (VI), 129.5 (I, VI'), 128.7 (V), 114.2 (VII), 106.7 (II), 74.9 (i), 70.8 (i'), 68.2 (1, y), 53.0 (x), 46.1 (f, g), 32.1 (10), 29.8 (2, 4 –

9), 26.3 (3), 22.8 (11), 14.3 (12).

FT-IR [Figure S1, cm^{-1}]: 2951 (ν (C–H) in $–CH_3$ (asymmetric)); 2920 – 2851 (ν (C–H) in $–CH_3$ (symmetric) and $–CH_2$- (asymmetric and symmetric)); 1613 (ν (C = O)); 1584 (ν (C = C–C aromatic)); 1512 (ν (C = C–C aromatic)); 1242 (ν (=C-O-C) asymmetric); 822 (δ (C–H) *p*-disubstitution).

2.4. Characterization techniques

2.4.1. Thermogravimetric analysis (TGA)

Thermal stability studies were carried out in ALU OXIDE crucibles of 70 μL (ME-24123) with a Mettler Toledo TGA2 thermobalance. All samples, weighing around 6 – 8 mg, were heated between 30 and 600 °C at a heating rate of 10 °C/min in N_2 atmosphere with a flow rate of 50 cm^3/min. The equipment was previously calibrated with indium (156.6 °C) and aluminum (660.3 °C) pearls.

2.4.2. Differential scanning calorimetry (DSC)

Calorimetric analyses were carried out on a Mettler DSC-821 instruments calibrated using indium (156.6 °C) and zinc (419.6 °C) pearls. Samples were placed in an aluminum standard crucible of 40 μL with pierced lids (between 4 and 6 mg of sample), which were analysed in N_2 atmosphere (gas flow rate of 50 cm^3/min). Heating and cooling rate of 10 °C/min was always employed.

2.4.3. Polarized optical microscopy (POM)

LC mesophases were investigated by polarized optical microscopy (POM). The textures of the samples were observed with an Axiolab Zeiss optical microscope equipped with a Linkam TP92 hot stage and a Moticam S6 digital camera.

2.4.4. Nuclear magnetic resonance (NMR) spectroscopy

All synthesized compounds were characterized by ^1H NMR and ^{13}C NMR spectra, which were recorded in deuterated chloroform ($CDCl_3$) with a Bruker Avance Neo 400 MHz spectrometer (^1H – 400 MHz; ^{13}C – 100.4 MHz) at RT (25 ± 5 °C). The chemical shifts were given in parts per million (ppm) from TMS (Tetramethylsilane) in ^1H NMR spectra, while the central peak of the solvent was taken as a reference in the case of ^{13}C NMR spectra.

2.4.5. Fourier transform infrared (FT-IR) spectroscopy

FT-IR spectra were recorded on an FT/IR-6700 spectrophotometer from JASCO in the wavelength range of 4000 – 400 cm^{-1} with a resolution of 4 cm^{-1} in the absorbance mode. This device is equipped with an attenuated total reflection accessory (ATR) with thermal control and a diamond crystal (Golden Gate heated single reflection diamond ATR from Specac-Teknokroma). The spectra were recorded at RT (25 ± 5 °C) from the solid-state pure compounds.

2.4.6. X-ray diffraction (XRD)

X-ray diffraction measurements (XRD) were made using a Bruker-AXS D8-Advance diffractometer with vertical θ-θ goniometer, incident- and diffracted-beam Soller slits of 2.5°, a fixed 0.5° receiving slit and an air-scattering knife on the sample surface. The angular 2θ range was between 2 and 40°. The data were collected with an angular step of 0.02° at a step/time of 0.5 s. Cukα radiation was obtained from a copper X-ray tube operated at 40 kV and 40 mA. Diffracted X-rays were detected with a PSD detector LynxEye-XE-T with an opening angle of 2.9°. The sample was placed inside an MTC-LOWTEMP chamber for in-situ temperature analysis.

2.4.7. Size exclusion chromatography (SEC)

Molecular weight analysis was performed via size exclusion chromatography (SEC) using an Agilent 1200 series system equipped with three serial columns (PLgel 3 μm MIXED-E, 5 μm PLgel MIXED-D and PLgel 20 μm MIXED-A from Polymer Laboratories) and an Agilent 1100 series refractive index detector working at 35 °C at a nominal flow rate of 1.0 mL/min with a sample concentration of 0.1 % w/w in tetrahydrofuran (THF) as solvent. The SEC system was calibrated using narrow polystyrene standards from Polymer Laboratories with molecular weights ranging from 500 to 400.000 Da.

3. Results and discussion

As mentioned in the introduction, the primary aim of this work was to synthetize a family of poly(2-(3,4,5-tris(4-dodecyloxybenzyloxy) phenyl)-2-oxazoline)s (PTOx) with different molecular weights from its monomer precursor TAPOx, through "living" cationic ring-opening polymerization (CROP) (Scheme 1). With this purpose, several conditions, such as solvent, concentration, temperature, initiator and terminating agent were tested (Table 1). The progress of the reaction (reaction time) was monitored by ^1H NMR.

In a typical polyoxazoline synthesis by CROP, we can differentiate three main steps: 1) initiation, which takes place by nucleophilic attack of the cyclic imino ether to the electrophilic initiator, forming the oxazolinium cation and triggering the polymerization; 2) propagation, in which the monomer is added to the on growing polyoxazoline backbone, and finally, 3) termination, which occurs via nucleophilic attack of an added terminating agent on the "living" cationic chain-end (Scheme 2) [30].

Since the first reported synthesis of a polyoxazoline by CROP, a broad number of initiators has been employed, including methyl, benzyl and acetyl halides, alkyl sulfonates, such as trifluoromethanesulfonates (triflates), *p*-toluenesulfonates (tosylates) and *p*-nitrobenzenesulfonates (nosylates), Lewis's acids, and oxazolinium salts [30,31]. More recently, other initiators have been explored: for instance, Klikovits and co-workers have reported the use of a photoacid generator as an initiator for the cationic photopolymerization of different 2-oxazolines [32].

In our case, we decided to first test benzyl bromide (BnBr) as an initiator (**Entry 1**). Unfortunately, the reaction did not take place and no polymer was observed by ^1H NMR within 10 days of reaction, showing that this initiator is not active enough to trigger the polymerization [33]. Therefore, we decided to change it to a more active initiator, an alkyl sulfonate-based initiator [34]. In this case, anhydrous benzotrifluoride (BTF) was chosen as a solvent (**Entries 2–3**), which is reported as environmentally less harmful than various conventional solvents, such as halogenated solvents and aromatic solvents [35]. In these reactions, we used MeOTs as an initiator, while two different monomer concentrations were employed in each of them. It was observed that the polymerization of TAPOx did not take place in the less concentrated Schlenk tube (**Entry 2**), although the polymerization reaction was successfully performed within 7 days when the monomer concentration was increased up to 0.5 M (**Entry 3**). Afterwards, we decided to carry out a reaction in bulk (**Entry 4**), inspired by a previously reported work by Percec and co-workers [36]. Nevertheless, the cleavage of the benzylic positions of the dendritic side group after 2 h was detected by NMR.

According to Hoogenboom and co-workers, the most appropriate temperature to polymerize 2-phenyl-2-oxazolines with MeOTs as an initiator was established at 130 °C [33,37]. In order to perform these experiments, we decided to change the solvent of the reaction to a higher boiling point one, since BTF has a boiling point of 102 °C. Therefore, we used *o*-dichlorobenzene (*o*-DCB), which has a boiling point of 180 °C. Hence, we decided to set up the reaction temperature at 130 °C with different monomer concentrations (0.5, 1.0 and 3.0 M). Unfortunately, in these attempts (**Entries 5–7**), the cleavage of the benzylic methylene of the dodecyloxybenzyloxy substituents of the side dendron was observed again. For this reason, we considered not to vary the monomer concentration, keeping it at 1.0 M from now on.

Concerning the reaction temperature, we explored the polymerization of PTOx at temperatures lower than 130 °C to avoid the cleavage of the benzylic positions. At the same time, we also used a more active

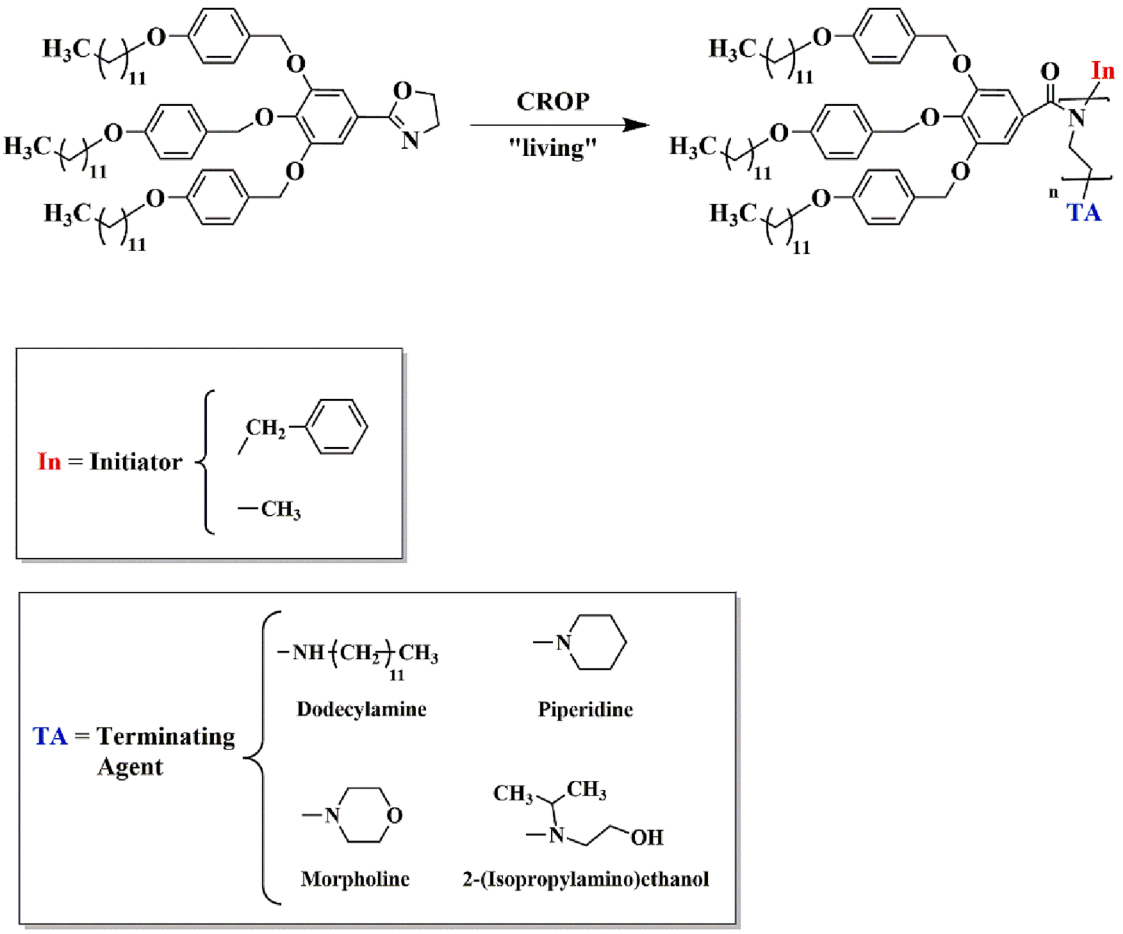

Scheme 1. Scheme of the "living" CROP of TAPOx.

initiator, methyl triflate [34,38], in order to obtain shorter reaction times. These reactions (**Entries 8–10**) were carried out at 110, 95 and 105 °C, respectively. Regarding the reaction that was carried out at 110 °C, the cleavage of the benzylic positions of the side dendron after 20 h of reaction was still detected. In contrast, the polymerization reaction at 95 °C proceeded successfully within 65 h; unfortunately, the terminating agent (dodecylamine) also provoked the cleavage of the benzylic methylene of the dodecyloxybenzyloxy substituents, when kept in the crude mixture for longer times (up to 16 h).

Consequently, we decided to change the terminating agent, from a

Table 1
Chemical reaction conditions and degrees of polymerization in the optimisation of the polymerization reaction of PTOx.

Entry	Initiator (mol %)	Solvent	T (°C)	Monomer concentration	Time	Terminating agent	Monomer conversion[a] (%)	Yield[b] (%)	EDP[c] (DP[d])
1	BnBr (1)	Toluene	90	0.1 M	10 days	–	–	–	100 (-)
2	MeOTs (1)	BTF[e]	95	0.2 M	10 days	–	–	–	100 (-)
3	MeOTs (5)	BTF	95	0.5 M	7 days	Dodecylamine	92	34	20 (7)
4	MeOTs (1)	Bulk	160	–	2 h	–	–	–	100 (-)
5	MeOTs (5)	*o*-DCB[f]	130	3.0 M	3 h	–	–	–	20 (-)
6	MeOTs (5)	*o*-DCB	130	1.0 M	5 h	–	–	–	20 (-)
7	MeOTs (5)	*o*-DCB	130	0.5 M	16 h	–	–	–	20 (-)
8	MeOTf (5)	*o*-DCB	110	1.0 M	20 h	–	–	–	20 (-)
9	MeOTf (5)	*o*-DCB	95	1.0 M	65 h	Dodecylamine	92	–	20 (-)
10	MeOTf (5)	*o*-DCB	105	1.0 M	44 h	Morpholine	93	43	20 (17)
11	MeOTf (5)	Chlorobenzene	105	1.0 M	30 h	Morpholine	96	64	20 (23)
12	MeOTf (5)	Chlorobenzene	105	1.0 M	29 h	Piperidine	93	–	20 (-)
13	MeOTf (5)	Chlorobenzene	105	1.0 M	30 h	2-(Isopropylamino) ethanol	94	–	20 (-)

[a] Estimated by ^{1}H NMR.
[b] % of polymer isolated after purification.
[c] EDP: Expected degree of polymerization.
[d] DP: Degree of polymerization estimated by ^{1}H NMR.
[e] BTF: Benzotrifluoride.
[f] *o*-DCB: *o*–Dichlorobenzene.

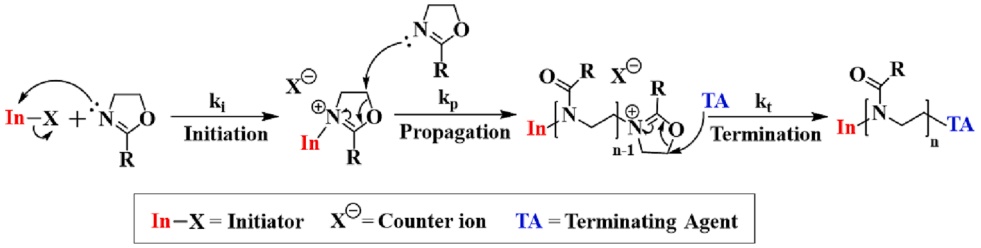

Scheme 2. General simplified mechanism of the CROP of 2-oxazolines.

primary amine to a more hindered secondary amine. Furthermore, the reaction was accelerated by increasing the temperature up to 105 °C as can be seen in **Entry 10**: in this way, it was successfully accomplished in 44 h, obtaining a pallid orange solution. In this case, morpholine was added as a terminating agent; and a polymer with a degree of polymerization equal to 17 (versus an expected one of 20) was obtained with a yield of 43 %. At this point, we decided to change the solvent, *o*-DCB, to a less polar one, i.e. chlorobenzene [39]. Using chlorobenzene, we noticed that reaction time was reduced from 44 h to 30 h, which agreed with the results previously reported by Monnery and co-workers [38]. Finally, other amine-based terminating agents were explored, piperidine and 2-(isopropylamino)ethanol. Unfortunately, they did not react as expected and, in addition, an increase of the side reactions was detected by ^{1}H NMR. Thus, the final degree of polymerization could not be estimated in these experiments.

In view of these results, we decided to choose the best reaction conditions as follows: 1.0 M concentration of TAPOx monomer, reaction temperature of 105 °C, MeOTf as an initiator, chlorobenzene as a solvent and morpholine as a terminating agent. In such conditions (**Entry 11**), a conversion of 96 % was obtained and the expected DP roughly coincides with the one estimated by ^{1}H NMR, which is in agreement with the expected "living" character of this polymerization. The degree of polymerization can be estimated from ^{1}H NMR spectra, by taking the signals of either initiator or terminating agent (or both) as a reference, and then compare their integrations with the integration of some signals assigned to the repeating units of the polymer. In our case, we decided to use only the terminating agent signals as a reference, since the signal of the initiator appeared overlapped with the polymer main chain signal in ^{1}H NMR spectra (3.42 – 4.03 ppm, Fig. 1). In fact, only the methylene adjacent to the nitrogen of the morpholine terminating agent, located at 2.35 ppm (Fig. 1), was used, since the methylene contiguous to the oxygen appeared also overlapped with the polymer main chain signal. The integration of this signal was compared with the integration of the signal that appears between 4.20 and 5.23 ppm, which is assigned to the benzylic methylene of the dodecyloxybenzyloxy substituents, and additionally with the integration of the signal that appear centred at 0.80, which correspond to the terminal methyl groups of the long aliphatic chain of the tapered side group (Fig. 1). The estimated DP from both comparisons was the same, in addition to agreeing with the expected DP as shown in Table 1. A more detailed explanation of NMR characterization of PTOx is reported in section 3.1.

After optimising all the parameters of the polymerization reaction, we decided to modify the percentage of initiator used in order to increase in a controlled manner the molecular weight of the polymers. To do so, the amount of initiator has to be reduced since we kept the amount of TAPOx constant (Table 2). The first noteworthy fact is that the reaction time slowly increased on reducing the initiator until 2.0 % (**Entries 11, 14–16)**. With amounts of initiator less than 2.0 %, the reaction time increased dramatically, as can be seen in **Entry 17**, in which 84 h were needed to reach a monomer conversion equal to 93 %. The variation of the viscosity of the reaction crude over time could delay the progress of the polymerization reaction.

Table 2 shows the monomer conversion and the obtained yields of the performed reactions. As estimated by ^{1}H NMR, monomer conversion was higher than 93 % in **Entries 11** and **14–17**, which makes the experimental DPs of the synthesized poly(2-oxazoline)s practically identical to the expected DPs (obtained from the monomer/initiator molar ratio). The narrow molecular weight distributions, estimated by SEC (Table 2), corroborated the expected "living" character exhibited by this polymerization, since dispersity values between 1.16 and 1.35 were obtained. When we tried to increase the expected DP beyond 80 units (**Entries 18–19**), the complete conversion of the monomer was not reached. In fact, we observed that there was about 25 – 28 % of TAPOx remaining unreacted, even after 5 – 6 days of reaction, which could not be separated from the formed poly(2-oxazoline)s during the purification process. Therefore, neither a real yield nor a degree of polymerization could be obtained in these cases. On the other hand, the yield of the polymerization reaction was generally between 63 and 75 %, indicating

Table 2
Chemical reaction conditions (% of initiator and reaction time), achieved conversion, expected and obtained degrees of polymerization and molecular parameters of the synthesized family of PTOx.

Entry	EDP[a]	Initiator (mol %)	Time (h)	Monomer conversion[b] (%)	Yield[c] (%)	DP[d]	M_n[e] (kDa)	M_w[f] (kDa)	Đ[f]
11	20	5.0	30	96	64	23	23.4	9.6	1.25
14	30	3.3	42	94	63	32	32.6	14.0	1.26
15	40	2.5	47	93	75	39	39.7	6.6	1.16
16	50	2.0	50	95	66	49	49.9	13.1	1.33
17	60	1.7	84	93	75	59	60.0	12.5	1.35
18	80	1.3	120	75	–	–	–	–	–
19	90	1.1	144	72	–	–	–	–	–

[a] EDP: Expected degree of polymerization.
[b] Estimated by ^{1}H NMR.
[c] % of polymer isolated after purification.
[d] DP: Degree of polymerization estimated by ^{1}H NMR.
[e] Molecular weight estimated by ^{1}H NMR.
[f] M_w and dispersity estimated by SEC.

that some amount of polymer was lost during the work-up process.

Moreover, the molecular weights of this family of polymers were also estimated by SEC, although no correlation between M_w or M_n was found (Figure S2). In our case, we used polystyrene patterns in SEC as a reference to calculate the molecular weight of these poly(2-oxazoline)s. Nevertheless, the hydrodynamic volume of this family of polymers is rather different from polystyrene, which is responsible of the lack of correlation between molecular weights estimated by ^{1}H NMR and SEC.

3.1. Chemical characterization

The chemical structure of PTOx was characterized by NMR and FT-IR spectroscopy.

As regards ^{1}H NMR, Fig. 1 shows the spectrum of PTOx40, which was performed using $CDCl_3$ as solvent. The first noticeable thing is that all ^{1}H NMR spectra are characterized by broad signals in three regions. We observe two broad peaks in the aromatic region between 6.25 and 7.34 ppm, which are the signals of the aromatic protons of the side chain dendron. When we move to lower frequencies, the first broad signal between 4.20 and 5.23 ppm is attributed to the benzylic methylenes of the dodecyloxybenzyloxy substituents. In the upfield region of the spectra, the peaks between 0.80 and 1.87 ppm are assigned to the aliphatic long chains of the dendron. These peaks are in agreement with the characterization of TAPOx monomer previously described by us [29]. The most interesting region is situated between 2.35 ppm and 4.03 ppm, since the peaks attributed to the protons of the polymer main chain, the morpholine terminating agent and the initiator appear in this area. In fact, the broad peak centred at 3.75 ppm is assigned to both methylenes of the poly(2-oxazoline) main chain (indexed as f and g in Fig. 1), the methylene contiguous to the oxygen of the long aliphatic side chains (1), the methylene of the initiator (s) and both methylenes contiguous to the oxygen of the morpholine terminating agent (y). In addition, the new broad peak centred at 2.35 ppm is attributed to both methylenes contiguous to the nitrogen of the terminating agent (x) in the final structure of the poly(2-oxazoline). This was confirmed by 2D NMR spectrum (COSY; Fig. 2). Moreover, the lack of both characteristic signals of the oxazoline ring, which are expected to appear at 4.34 and 3.97 ppm respectively, confirms a complete monomer conversion [29].

Fig. 3 shows the ^{13}C NMR spectrum of PTOx40 with the corresponding assignments. First of all, the signal at 171.8 ppm is attributed to the carbonyl carbon of the amide of each side dendron (indexed with the letter q in Fig. 3), whereas the signals between 106.7 and 158.9 ppm belong to the aromatic carbons of the dendronized side chain of the poly (2-oxazoline). In the aliphatic region, two signals observed at 74.9 and 70.8 ppm are assigned to the carbons of the benzylic methylenes of the central and lateral dodecyloxybenzyloxy substituents of each dendron, respectively. Moving upfield in the spectrum, the peak at 68.2 ppm is attributed to the methylenic carbons contiguous to the oxygen of the long aliphatic side chains together with the methylenic carbons contiguous to the oxygen of the morpholine terminating agent. In addition, the small peak observed at 53.6 ppm belongs to both methylenic carbons contiguous to nitrogen of morpholine, thus confirming that the terminating agent was successfully incorporated in the final polymer structure. Besides, the small broad peak at 46.1 ppm is

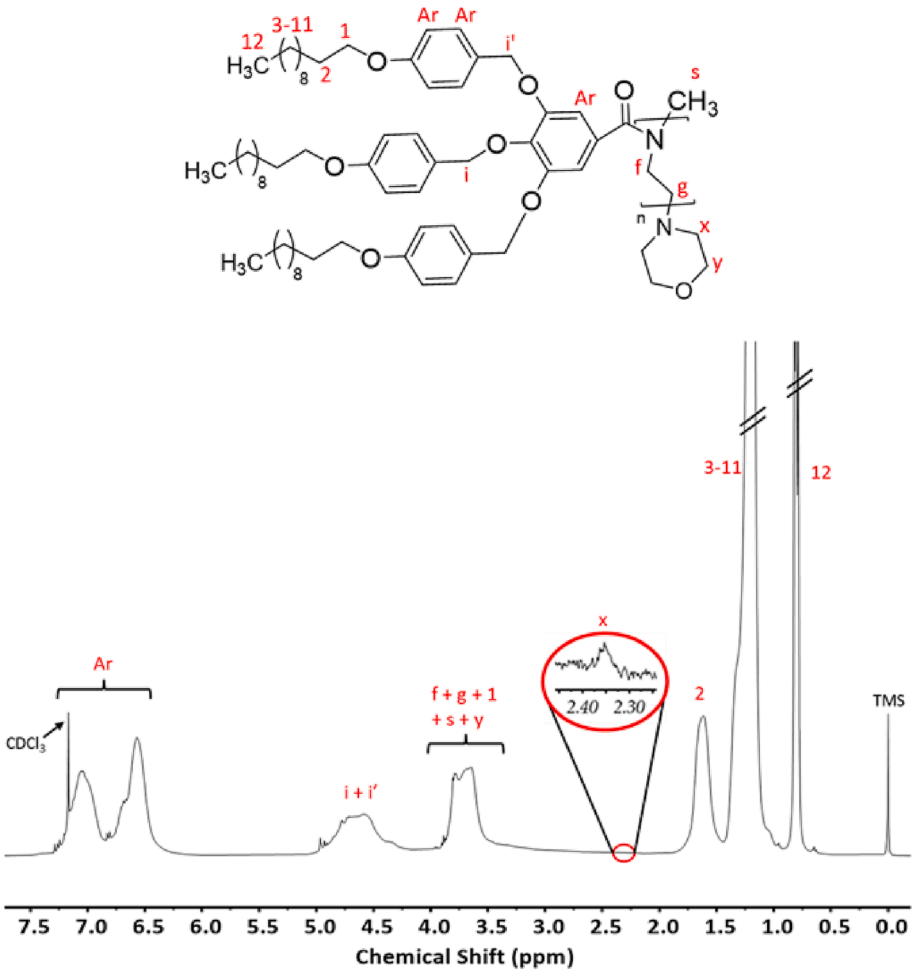

Fig. 1. ^{1}H NMR spectrum of PTOx40 in $CDCl_3$.

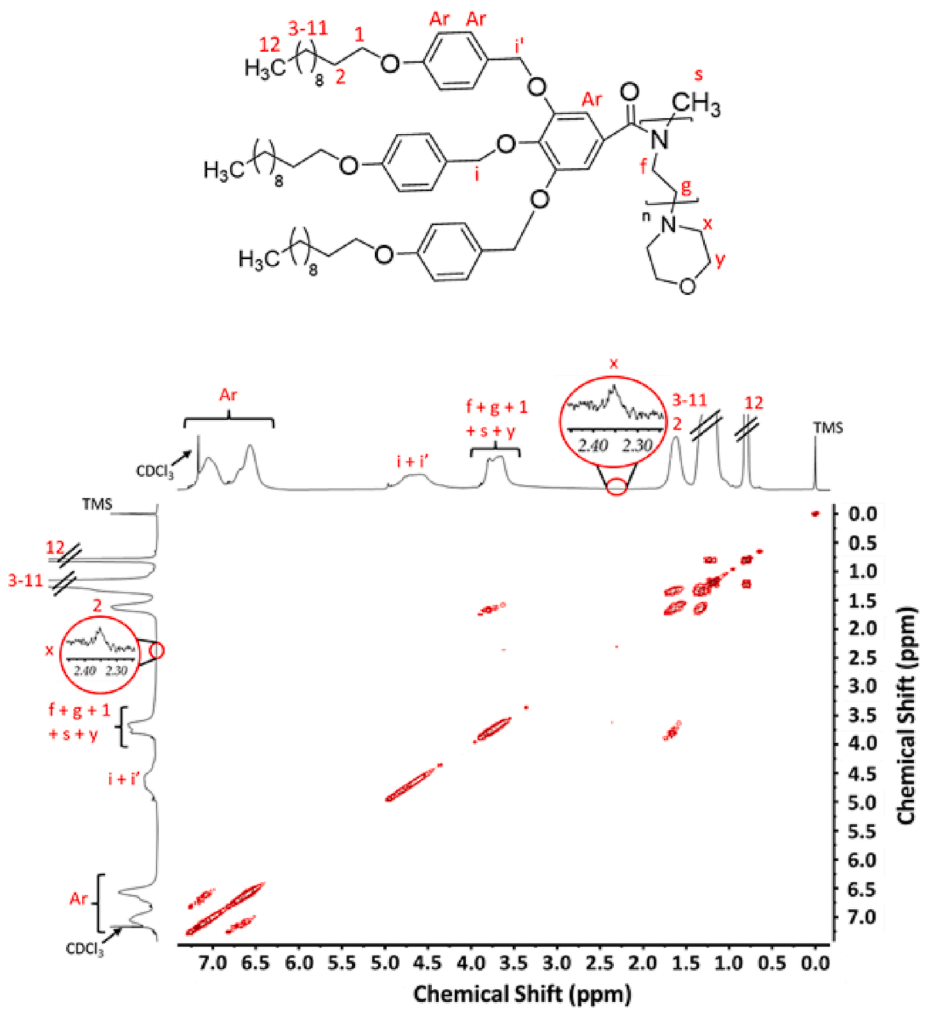

Fig. 2. COSY NMR spectrum of PTOx40.

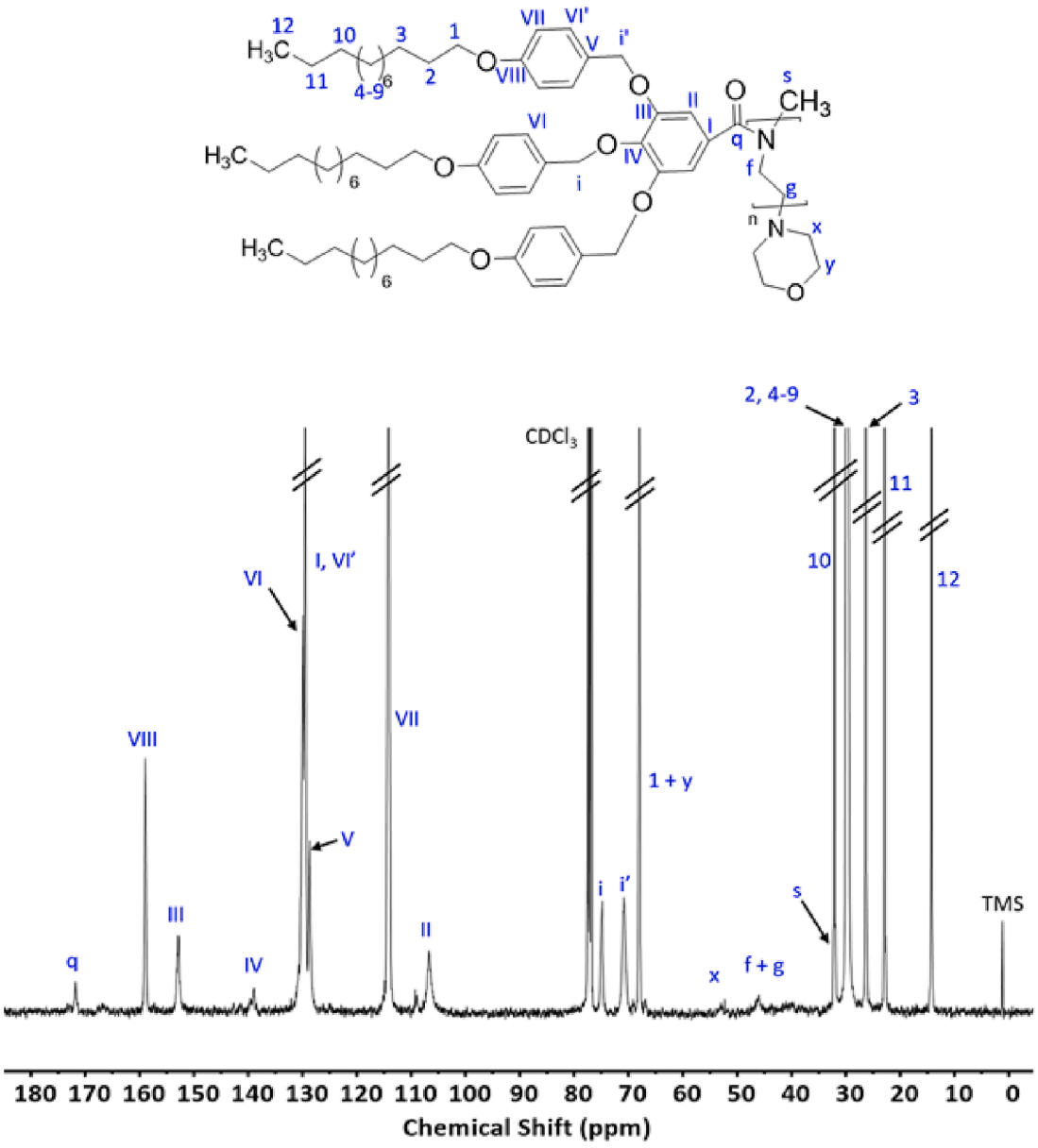

Fig. 3. ^{13}C NMR spectrum of PTOx40 in $CDCl_3$.

attributed to the carbons of the main chain of the acyl-substituted poly (ethyleneimine) (f and g). This peak, as well as the absence of the peaks assigned to the methylenic carbons of the oxazoline ring expected at 67.9 and 55.0 ppm respectively, corroborate that TAPOx monomer was completely consumed during the CROP [29]. Finally, all the peaks between 32.1 and 14.3 ppm are assigned to the carbons of the aliphatic side chain of the dendrons (2–12). This information agrees with the previously reported characterization of the TAPOx monomer [29].

Moreover, PTOx40 structure was also characterized by means of FT-IR spectroscopy (Figure S1). Thus, the FT-IR spectrum of this poly(2-oxazoline) shows an intense band at 1613 cm^{-1}, which is attributed to the C = O stretching vibration of the amide carbonyl group. This band was also detected when we recorded the FT-IR of *N*-(2-hydroxyethyl)-3,4,5-tris(4-dodecyloxybenzyloxy)benzamide (TAPAm), the dendritic amide precursor synthesized in the reported pathway to obtain TAPOx [29]. Furthermore, total monomer conversion was also certified by the complete disappearance of the stretching vibration band typical of 2-oxazolines (1643 cm^{-1} in FT-IR spectrum of TAPOx monomer, Figure S1) [40].

3.2. Thermal and mesomorphic characterization

Thermal and mesomorphic characterization of the members of the PTOx family was performed by DSC, TGA, POM and XRD experiments. Table 3 shows calorimetric data of the whole PTOx family.

As represented in Fig. 4, DSC thermograms reveal the presence of a glass transition temperature between −16 and −12 °C for all side chain liquid crystalline poly(2-oxazoline)s synthesized. Furthermore, a small

Table 3
Calorimetric features of the PTOx family.

PTOx	T_g (°C)[a]	T_c (°C)[a]	$T_{5\%}$ (°C)	ΔH (kJ/mol)[b]
PTOx20	−13	81	282	1.1
PTOx30	−15	–	288	–
PTOx40	−12	80[c]	287	1.2[c]
PTOx50	−14	–	290	–
PTOx60	−16	–	287	–

[a] Determined by DSC first heating scan.
[b] Expressed per mol of tapered repeating unit.
[c] Determined by DSC second heating scan.

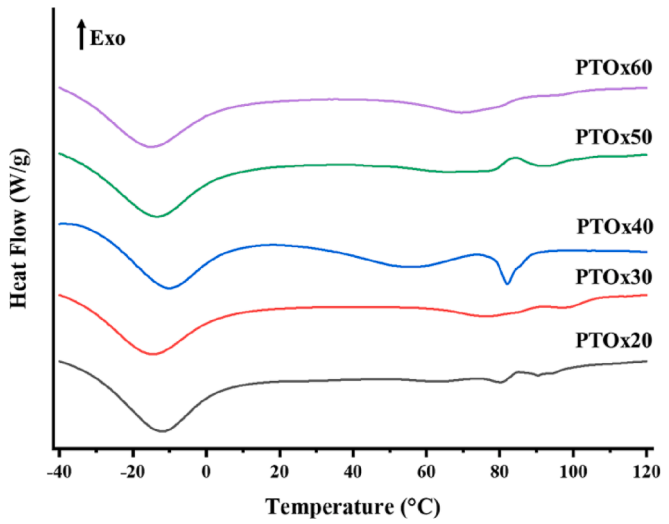

Fig. 4. Calorimetric analysis of all synthesized PTOx; DSC first heating scan of: PTOx20, PTOx30, PTOx40, PTOx50 and PTOx60 (Scan rate: 10 °C/min).

endotherm centred at 81 and 80 °C was observed in the case of PTOx20 and PTOx40, respectively. Moreover, POM experiments put into evidence that this endotherm corresponds to the clearing temperatures (T_c) of the dendronized polymers, since an isotropic viscous liquid was observed above it. This endotherm could be only detected by DSC in the first heating for PTOx20 and PTOx40, while no exotherm was observed on cooling from the molten state of these polymers except for PTOx40 (T_c was also not detected by DSC second heating scan except for PTOx40). Nevertheless, it was possible to see by POM how different LC textures grew on cooling to RT after 24 h of annealing at 74 °C (Fig. 5a and c). Besides, a small shoulder just after the endotherm at 80 °C could be seen for some SCLC poly(2-oxazoline)s, which corresponds to an endothermic peak. As the XRD studies demonstrated, this endotherm was not attributed to a thermal transition between different LC mesophases (Figure S3); suggesting that a hysteresis phenomenon occurs in this temperature range.

Unlike the other members of the family, PTOx40 showed an exotherm at 64 °C on cooling, which was attributed to the anisotropization temperature (Figure S4). Besides, a shoulder that appears overlapped with the endotherm associated to the T_c in the DSC first heating scan is not detected in the second heating scan, allowing to determine both the T_c and the associated enthalpy in a more accurate way. In this case, the LC mesophase was also observed by POM during both heating and cooling, confirming the thermal transitions previously detected by DSC. As observed in Fig. 5b, a pseudo-focal conic fan-shaped texture typical of these mesogens was exhibited by PTOx40.

The associated enthalpies to the clearing transitions of PTOx20 and PTOx40 (Table 3) roughly coincide with the already reported enthalpies for systems that self-assemble into hexagonal columnar (Col_h) lattices [26,36,41].

For the purpose to confirm calorimetric features and to assign the LC mesophases of the synthesized poly(2-oxazoline)s, X-ray diffraction analysis were carried out at different temperatures (Figs. 6 and 7). As reported in Table 4, the investigated PTOx presented columnar mesophases (*Col*), as expected. Actually, Percec and co-workers established that the columnar self-assembly of this type of hemiphasmidic polymers is driven mainly by supramolecular interactions (π-π interactions) of the aromatic moieties present in tapered side chain dendrons. Thanks to these interactions, these dendritic side-groups can induce a helical arrangement of the polymer chain into columns [42,43].

Below the T_c, the X-ray diffractograms of PTOx show a sharp peak located in the ranges of 2θ angles 2.2 – 2.3° (corresponding to d-spacings between 38.6 and 39.3 Å), and a broad halo centred around 2θ = 19.2 – 19.5° (which corresponds to d-spacings between 4.5 and 4.6 Å). The higher spacing seen in the XRD pattern should correspond to the lateral distance between columns, while the lower spacing might be attributed to the planar distance between dendrons, as we have previously reported for SCLCPs that contain this dendritic side group and self-assemble into columnar structures [23,24,26,44,45]. Regarding PTOx40, its XRD

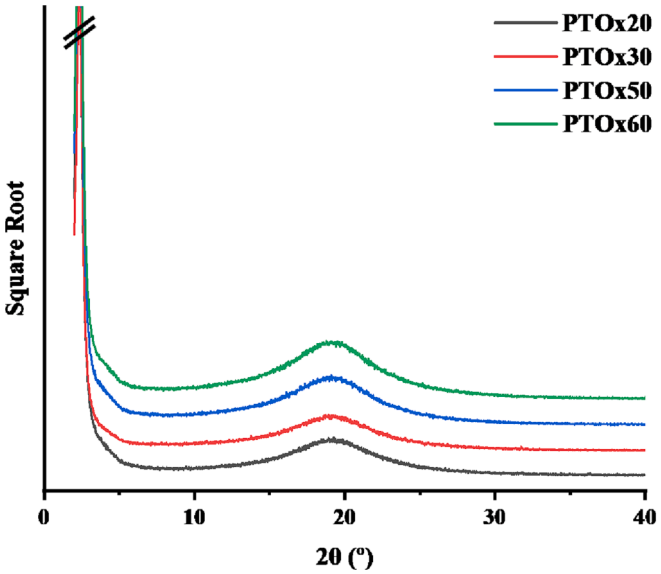

Fig. 6. X-ray diffractograms of PTOx20, PTOx30, PTOx50 and PTOx60 recorded at 50 °C.

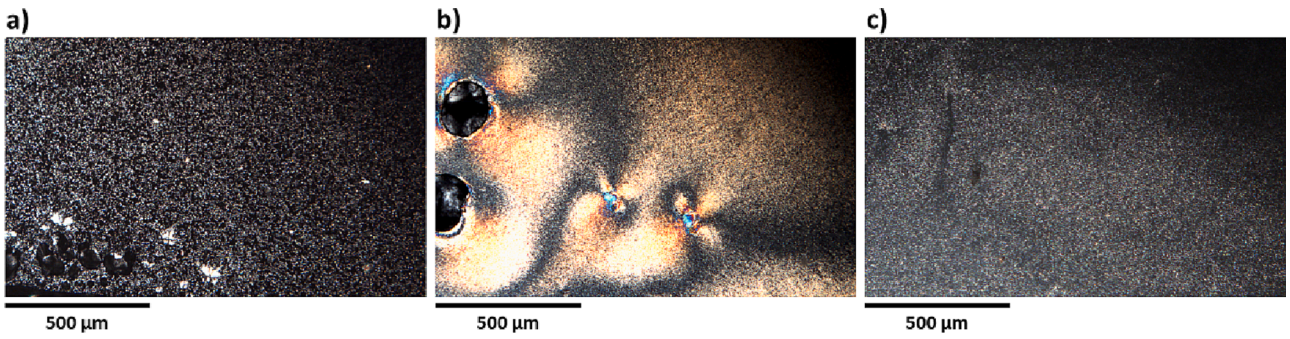

Fig. 5. Optical micrographs between crossed polars of: (a) PTOx20, (b) PTOx40 and (c) PTOx60 recorded at RT (25 ± 5 °C) on cooling from isotropization. In the case of PTOx20 and PTOx60, pictures were taken after annealing at 74 °C during 24 h and then cooling the poly(2-oxazoline)s to RT.

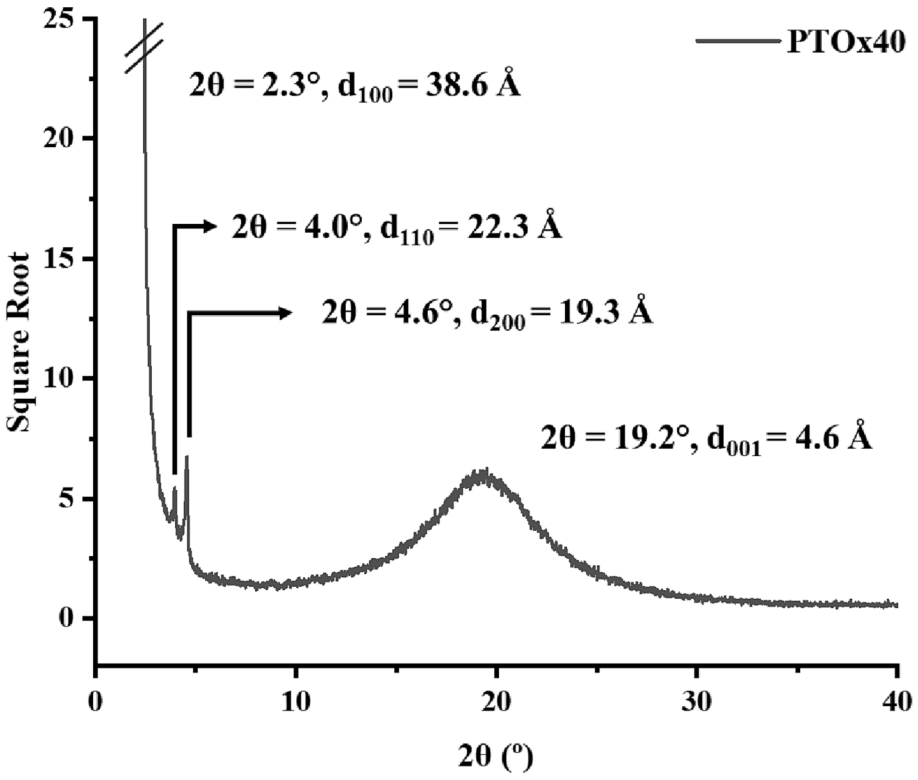

Fig. 7. X-ray diffractogram of PTOx40 recorded at 60 °C.

Table 4
XRD diffraction data of PTOx family.

PTOx[a]	d_{100} (Å)	d_{110} (Å)	d_{200} (Å)	d_{001} (Å)	a (Å)	Mesophase[b]
PTOx20	39.3	–	–	4.6	–	*Col*
PTOx30	38.9	–	–	4.6	–	*Col*
PTOx40	38.6	22.3	19.3	4.6	44.6	Col_h
PTOx50	38.6	–	–	4.5	–	*Col*
PTOx60	38.9	–	–	4.5	–	*Col*

[a] X-ray diffractograms of PTOx20, PTOx30, PTOx50 and PTOx60 were recorded at 50 °C, while X-ray diffractogram of PTOx40 was recorded at 60 °C.
[b] *Col*: columnar. Col_h: hexagonal columnar.

diffractogram presents three sharp reflections centred at 2θ = 2.3° (d = 38.6 Å), 3.9° (d = 22.3 Å) and 4.6° (d = 19.3 Å). The relationship between these d-spacings, which is equal to $1:1/\sqrt{3}:1/2$, together with the presence of the diffuse halo centered at 2θ = 19.3° (d = 4.6 Å) confirms the existence of a hexagonal columnar mesophase (Col_h). Thus, the sharp reflections are assigned to the lattice planes indexed as (1 0 0), (1 1 0) and (2 0 0), respectively, while the broad halo corresponds to the plane (0 0 1). In all cases, the columnar organization of these dendronized poly (2-oxazoline)s suggests that their main chains could arrange forming biomimetic ion channels.

Thermal stability of all the members of the PTOx family was studied by TGA. As can be seen in Fig. 8, this family of dendronized poly(2-oxazoline)s presents the same thermal stability pattern. All these liquid crystalline polymers present an onset of thermal weight loss (determined as the temperature corresponding to 5 % mass loss) in the range between 282 and 290 °C (Table 3) and a remaining char yield between 15 and 17 % at 600 °C. Moreover, the DGTA curves of these dendronized poly(2-oxazoline)s evidenced that their thermal degradation occurs *via* two-step weight loss (Figure S5). This data agrees with the information reported in literature during the last years for 2-phenyl-oxazoline based polymers, which exhibited complex decomposition mechanisms [46,47].

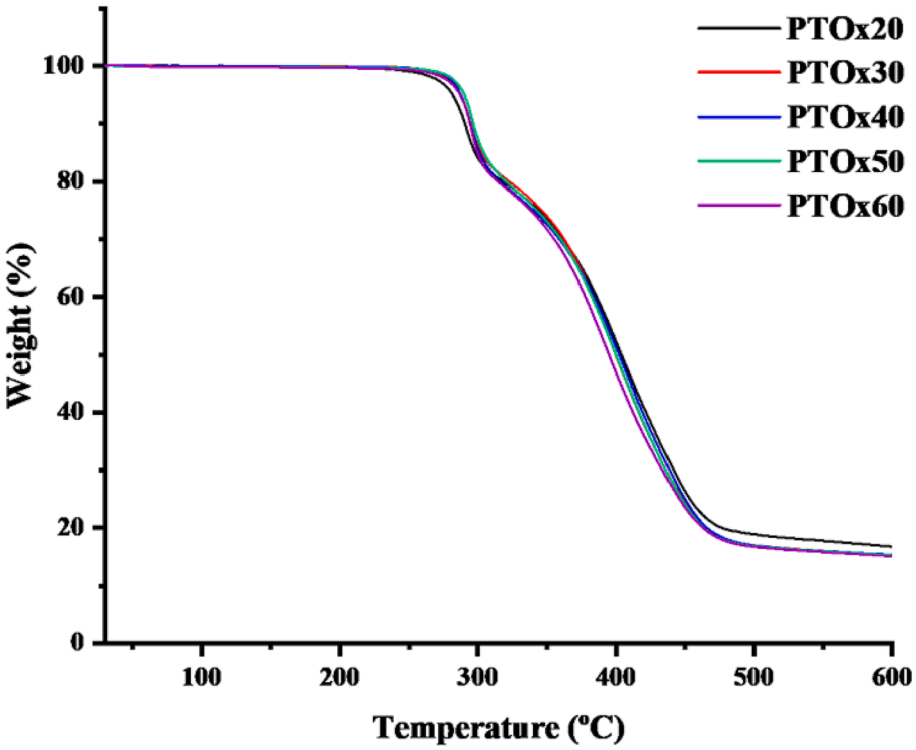

Fig. 8. TGA thermogram of PTOx family recorded at a heating rate of 10 °C/min in nitrogen atmosphere.

4. Conclusions

A new family of poly(*N*-acylethyleneimine)s has been successfully synthetized by "living" CROP of dendronized TAPOx, obtaining poly(2-oxazoline)s within a range of molecular weights between 20 and 60 kDa. Early investigations suggest that several factors affect the polymerization reaction of TAPOx: temperature, type of initiator, monomer concentration, terminating agent and solvent. Concerning the reaction temperature, our studies showed that a compromise between time and temperature was necessary to avoid the cleavage of the benzylic positions of the side dendron. When the reactions were carried out above 105 °C, this cleavage occurred; on the other hand, working at lower temperatures determined too long reaction times. Therefore, the optimal temperature to perform this CROP is 105 °C. With respect to the initiator, methyl based initiators such as MeOTs and MeOTf allowed the obtention of dendronized poly(2-oxazoline)s, even though the polymerizations carried out with MeOTf showed shorter reaction times as expected. Therefore, these studies allowed tuning the optimal polymerization conditions, which resulted the following: reaction temperature equal to 105 °C, use of MeOTf as an initiator, chlorobenzene as a solvent, morpholine as a terminating agent, while the monomer concentration was fixed at 1.0 M.

The liquid crystalline character of these poly(*N*-acylethyleneimine)s was investigated. Calorimetric studies showed that the entire family of PTOx exhibited liquid crystalline behaviour. In fact, the liquid crystalline mesophases of these poly(2-oxazoline)s, which could be evidenced by DSC, present a wide range of temperature (*ca* 90 °C), exhibiting the liquid crystalline mesophase already at RT (25 ± 5 °C). Nevertheless, this mesophase could be only observed by DSC on the first heating scan for all PTOx except for PTOx40, which showed a clear enantiotropic liquid crystalline mesophase. On the other hand, POM experiments proved that LC mesophases of PTOx20-30 and PTOx50-60 could be grown on cooling after annealing at 74 °C during 24 h. XRD analysis showed that the entire family of poly(2-oxazoline)s self-assembles into columnar mesophases, being able to detect a hexagonal columnar mesophase in the case of PTOx40. All these results evidenced that these novel family of SCLC acyl-substituted poly(ethyleneimine)s could be promising materials with the ability to transport diverse cations in the development of new biomimetic membranes.

CRediT authorship contribution statement

Jordi Guardià: Formal analysis, Investigation, Methodology, Validation, Writing – original draft. **Marta Giamberini:** Data curation, Funding acquisition, Resources, Validation. **José Antonio Reina:** Conceptualization, Data curation, Formal analysis, Funding acquisition, Project administration, Resources, Supervision, Validation, Writing – review & editing. **Xavier Montané:** Conceptualization, Data curation, Formal analysis, Funding acquisition, Investigation, Methodology, Project administration, Resources, Supervision, Validation, Writing – original draft, Writing – review & editing.

Declaration of Competing Interest

The authors declare that they have no known competing financial interests or personal relationships that could have appeared to influence the work reported in this paper.

Data availability

Data will be made available on request.

Acknowledgements

This work was supported by the Ministerio de Ciencia e Innovación (España), grant number PID2020-116322RB-C32. This project has received funding from the European Union's Horizon 2020 research and innovation programme under the Marie Skłodowska-Curie grant agreement No. 713679.

The authors are grateful to Francesc Gispert for his help in XRD experiments and Ramon Guerrero for his help in NMR experiments (Scientific & Technical Resources Service, Universitat Rovira i Virgili).

Appendix A. Supplementary material

Supplementary data to this article can be found online at https://doi.org/10.1016/j.eurpolymj.2023.112273.

References

[1] H. Zhang, P.K. Shen, Recent development of polymer electrolyte membranes for fuel cells, Chem. Rev. 112 (2012) 2780–2832, https://doi.org/10.1021/cr200035s.

[2] A.K. Sahu, G. Selvarani, S. Pitchumani, P. Sridhar, A.K. Shukla, A Sol-Gel Modified Alternative Nafion-Silica Composite Membrane for Polymer Electrolyte Fuel Cells, J. Electrochem. Soc. 154 (2007) B123–B132, https://doi.org/10.1149/1.2401031.

[3] G. Hernández-Flores, H.M. Poggi-Varaldo, O. Solorza-Feria, Comparison of alternative membranes to replace high cost Nafion ones in microbial fuel cells, Int. J. Hydrog. Energy. 41 (2016) 23354–23362, https://doi.org/10.1016/j.ijhydene.2016.08.206.

[4] M. Schadt, Photo alignment and patterning of liquid crystal polymer films and optical devices by side-chain photopolymers, Mol. Cryst. Liq. Cryst. 594 (2014) 11–20, https://doi.org/10.1080/15421406.2014.917456.

[5] J.R. Werber, C.O. Osuji, M. Elimelech, Materials for next-generation desalination and water purification membranes, Nat. Rev. Mater. 1 (2016) 1–15, https://doi.org/10.1038/natrevmats.2016.18.

[6] M. Zhou, P.R. Nemade, X. Lu, X. Zeng, E.S. Hatakeyama, R.D. Noble, D.L. Gin, New type of membrane material for water desalination based on a cross-linked bicontinuous cubic lyotropic liquid crystal assembly, J. Am. Chem. Soc. 129 (2007) 9574–9575, https://doi.org/10.1021/ja073067w.

[7] T. Kato, M. Yoshio, T. Ichikawa, B. Soberats, H. Ohno, M. Funahashi, Transport of ions and electrons in nanostructured liquid crystals, Nat. Rev. Mater. 2 (2017) 17001, https://doi.org/10.1038/natrevmats.2017.1.

[8] J. Sakuda, E. Hosono, M. Yoshio, T. Ichikawa, T. Matsumoto, H. Ohno, H. Zhou, T. Kato, Liquid-crystalline electrolytes for lithium-ion batteries: Ordered assemblies of a mesogen-containing carbonate and a lithium salt, Adv. Funct. Mater. 25 (2015) 1206–1212, https://doi.org/10.1002/adfm.201402509.

[9] W. Seeliger, E. Aufderhaar, W. Diepers, R. Feinauer, R. Nehring, W. Thier, H. Hellmann, Recent Syntheses and Reactions of Cyclic Imidic Esters, Angew. Chem. Int. Ed. Engl. 5 (1966) 875–888, https://doi.org/10.1002/anie.196608751.

[10] D.A. Tomalia, D.P. Sheetz, Homopolymerization of 2-alkyl- and 2-aryl-2-oxazolines, J. Polym. Sci., Part A-1, Polym. Chem. 4 (1966) 2253–2265, https://doi.org/10.1002/pol.1966.150040919.

[11] T. Kagiya, S. Narisawa, T. Maeda, K. Fukui, Ring-opening polymerization of 2-substituted 2-oxazolines, J. Polym. Sci., Part B: Polym. Lett. 4 (1966) 441–445, https://doi.org/10.1002/pol.1966.110040701.

[12] T.G. Bassiri, A. Levy, M. Litt, Polymerization of cyclic imino ethers. I. Oxazolines, J. Polym. Sci., Part B: Polym. Lett. 5 (1967) 871–879, https://doi.org/10.1002/pol.1967.110050927.

[13] B. Guillerm, S. Monge, V. Lapinte, J.J. Robin, How to modulate the chemical structure of polyoxazolines by appropriate functionalization, Macromol. Rapid Commun. 33 (2012) 1600–1612, https://doi.org/10.1002/marc.201200266.

[14] V. Mazánková, P. Sťahel, P. Matoušková, A. Brablec, J. Čech, L. Prokeš, V. Buršíková, M. Stupavská, M. Lehocký, K. Ozaltin, P. Humpolíček, D. Trunec, Atmospheric pressure plasma polymerized 2-ethyl-2-oxazoline based thin films for biomedical purposes, Polymers (Basel) 12 (2020) 2679, https://doi.org/10.3390/polym12112679.

[15] M.N. Ramiasa, A.A. Cavallaro, A. Mierczynska, S.N. Christo, J.M. Gleadle, J. D. Hayball, K. Vasilev, Plasma polymerised polyoxazoline thin films for biomedical applications, Chem. Comm. 51 (2015) 4279–4282, https://doi.org/10.1039/c5cc00260e.

[16] X. Liu, J. Yuan, J. Zhang, R.M. Visalakshan, W. Wang, Y. Xiang, Y. He, Q. Feng, K. Vasilev, The introduction of nanotopography suppresses bacterial adhesion and enhances osteoinductive capacity of plasma deposited polyoxazoline surface, Mater. Lett. 309 (2022), 131452, https://doi.org/10.1016/j.matlet.2021.131452.

[17] M.J. Sánchez-Fernández, J. Rutjes, R.P. Félix Lanao, J.C.M.E. Bender, J.C.M. van Hest, S.C.G. Leeuwenburgh, Bone-Adhesive Hydrogels Based on Dual Crosslinked Poly(2-oxazoline)s, Macromol. Biosci. 21 (2021) 2100257, https://doi.org/10.1002/mabi.202100257.

[18] R. Konradi, C. Acikgoz, M. Textor, Polyoxazolines for nonfouling surface coatings - A direct comparison to the gold standard PEG, Macromol. Rapid Commun. 33 (2012) 1663–1676, https://doi.org/10.1002/marc.201200422.

[19] O. Sedlacek, O. Janouskova, B. Verbraeken, R. Hoogenboom, Straightforward Route to Superhydrophilic Poly(2-oxazoline)s via Acylation of Well-Defined Polyethylenimine, Biomacromolecules. 20 (2019) 222–230, https://doi.org/10.1021/acs.biomac.8b01366.

[20] J. Svoboda, O. Sedláček, T. Riedel, M. Hrubý, O. Pop-Georgievski, Poly(2-oxazoline)s One-Pot Polymerization and Surface Coating: From Synthesis to Antifouling Properties Out-Performing Poly(ethylene oxide), Biomacromolecules. 20 (2019) 3453–3463, https://doi.org/10.1021/acs.biomac.9b00751.

[21] J.M. Rodriguez-Parada, V. Percec, Synthesis and characterization of liquid crystalline poly(N-acylethyleneimine)s, J. Polym. Sci., Part A: Polym. Chem. 25 (1987) 2269–2279, https://doi.org/10.1002/pola.1987.080250823.

[22] V. Percec, M.N. Holerca, S. Uchida, D.J.P. Yeardley, G. Ungar, Poly(oxazoline)s with tapered minidendritic side groups as models for the design of synthetic macromolecules with tertiary structure. A demonstration of the limitations of living polymerization in the design of 3-D structures based on single polymer chains, Biomacromolecules. 2 (2001) 729–740, https://doi.org/10.1021/bm015559l.

[23] S.V. Bhosale, M.A. Rasool, J.A. Reina, M. Giamberini, New liquid crystalline columnar poly(epichlorohydrin-co-ethylene oxide) derivatives leading to biomimetic ion channels, Polym. Eng. Sci. 53 (2013) 159–167, https://doi.org/10.1002/pen.23240.

[24] X. Montané, S.V. Bhosale, J.A. Reina, M. Giamberini, Columnar liquid crystalline polyglycidol derivatives: A novel alternative for proton-conducting membranes, Polymer (Guildf). 66 (2015) 100–109, https://doi.org/10.1016/j.polymer.2015.03.071.

[25] A. Šakalyte, J.A. Reina, M. Giamberini, Liquid crystalline polyamines containing side dendrons: Toward the building of ion channels based on polyamines, Polymer (Guildf). 54 (2013) 5133–5140, https://doi.org/10.1016/j.polymer.2013.07.027.

[26] X. Montané, K.A. Bogdanowicz, G. Colace, J.A. Reina, P. Cerruti, A. Lederer, M. Giamberini, Advances in the design of self-supported ion-conducting membranes-new family of columnar liquid crystalline polyamines. Part 1: Copolymer synthesis and membrane preparation, Polymer (Guildf). 105 (2016) 298–309. https://doi.org/10.1016/j.polymer.2016.10.047.

[27] X. Montané, K.A. Bogdanowicz, J. Prats-Reig, G. Colace, J.A. Reina, M. Giamberini, Advances in the design of self-supported ion-conducting membranes – New family of columnar liquid crystalline polyamines. Part 2: Ion transport characterisation and comparison to hybrid membranes, Polymer (Guildf). 105 (2016) 234–242, https://doi.org/10.1016/j.polymer.2016.10.046.

[28] D.D. Perrin, W.L.F. Armarego, Purification of laboratory chemicals, Pergamon Press, 2009.

[29] J. Guardià, A. Zare, J. Eleeza, M. Giamberini, J.A. Reina, X. Montané, Synthesis and characterization of dendritic compounds containing nitrogen: monomer precursors in the construction of biomimetic membranes, Sci. Rep. 12 (2022) 1725, https://doi.org/10.1038/s41598-022-05747-1.

[30] B. Verbraeken, B.D. Monnery, K. Lava, R. Hoogenboom, The chemistry of poly(2-oxazoline)s, Eur. Polym. J. 88 (2017) 451–469, https://doi.org/10.1016/j.eurpolymj.2016.11.016.

[31] M. Glassner, M. Vergaelen, R. Hoogenboom, Poly(2-oxazoline)s: A comprehensive overview of polymer structures and their physical properties, Polym. Int. 67 (2018) 32–45, https://doi.org/10.1002/pi.5457.

[32] N. Klikovits, L. Sinawehl, P. Knaack, T. Koch, J. Stampfl, C. Gorsche, R. Liska, UV-Induced Cationic Ring-Opening Polymerization of 2-Oxazolines for Hot Lithography, ACS Macro Lett. 9 (2020) 546–551, https://doi.org/10.1021/acsmacrolett.0c00055.

[33] R. Hoogenboom, M.W.M. Fijten, U.S. Schubert, The Effect of Temperature on the Living Cationic Polymerization of 2-Phenyl-2-oxazoline Explored Utilizing an Automated Synthesizer, Macromol. Rapid Commun. 25 (2004) 339–343, https://doi.org/10.1002/marc.200300233.

[34] M. Glassner, D.R. D'Hooge, J. Young Park, P.H.M. van Steenberge, B.D. Monnery, M.F. Reyniers, R. Hoogenboom, Systematic investigation of alkyl sulfonate initiators for the cationic ring-opening polymerization of 2-oxazolines revealing optimal combinations of monomers and initiators, Eur. Polym. J. 65 (2015) 298–304, https://doi.org/10.1016/j.eurpolymj.2015.01.019.

[35] B. Pásztói, T.M. Trötschler, Á. Szabó, B. Kerscher, H. Tenhu, R. Mülhaupt, B. Iván, Quasiliving cationic ring-opening polymerization of 2-ethyl-2-oxazoline in benzotrifluoride, as an alternative reaction medium, Polymer (Guildf). 212 (2021), 123165, https://doi.org/10.1016/j.polymer.2020.123165.

[36] V. Percec, M.N. Holerca, S.N. Magonov, D.J.P. Yeardley, G. Ungar, H. Duan, S. D. Hudson, Poly(oxazolines)s with tapered minidendritic side groups. The simplest cylindrical models to investigate the formation of two-dimensional and three-dimensional order by direct visualization, Biomacromolecules. 2 (2001) 706–728, https://doi.org/10.1021/bm015550j.

[37] R. Hoogenboom, R.M. Paulus, M.W.M. Fijten, U.S. Schubert, Concentration effects in the cationic ring-opening polymerization of 2-ethyl-2-oxazoline in N, N-dimethylacetamide, J. Polym. Sci., Part A: Polym. Chem. 43 (2005) 1487–1497, https://doi.org/10.1002/pola.20603.

[38] B.D. Monnery, S. Shaunak, M. Thanou, J.H.G. Steinke, Improved synthesis of linear poly(ethylenimine) via low-temperature polymerization of 2-isopropyl-2-oxazoline in chlorobenzene, Macromolecules. 48 (2015) 3197–3206, https://doi.org/10.1021/acs.macromol.5b00437.

[39] M. Vergaelen, B.D. Monnery, V.V. Jerca, R. Hoogenboom, Detailed Understanding of Solvent Effects for the Cationic Ring-Opening Polymerization of 2-Ethyl-2-oxazoline, Macromolecules. (2023), https://doi.org/10.1021/acs.macromol.2c01930.

[40] T. Kagiya, T. Matsuda, Selective Polymerization of 2-Isopropenyl-2-oxazoline and Cross-linking Reaction of the Polymers, Polym. J. 3 (1972) 307–314, https://doi.org/10.1295/polymj.3.307.

[41] V. Percec, C.-H. Ahn, W.-D. Cho, A.M. Jamieson, J. Kim, T. Leman, M. Schmidt, M. Gerle, M. Mo, S.A. Prokhorova, S.S. Sheiko, S.Z.D. Cheng, | A Zhang, | G Ungar, D. J.P. Yeardley, Visualizable Cylindrical Macromolecules with Controlled Stiffness from Backbones Containing Libraries of Self-Assembling Dendritic Side Groups, J. Am. Chem. Soc. 120 (1998) 8619–8631. https://doi.org/10.1021/ja981211v.

[42] V. Percec, M. Glodde, T.K. Bera, Y. Miura, I. Shiyanovskaya, K.D. Singer, V.S. K. Balagurusamy, P.A. Heiney, I. Schnell, A. Rapp, H.W. Spiess, S.D. Hudsonk, H. Duan, Self-organization of supramolecular helical dendrimers into complex electronic materials, Nature. 417 (2002) 384–387, https://doi.org/10.1038/nature01072.

[43] M. Peterca, D. Sahoo, M.R. Imam, Q. Xiao, V. Percec, Searching for the simplest self-assembling dendron to study helical self-organization and supramolecular polymerization, Giant. 12 (2022), 100118, https://doi.org/10.1016/j.giant.2022.100118.

[44] K.A. Bogdanowicz, G.A. Rapsilber, J.A. Reina, M. Giamberini, Liquid crystalline polymeric wires for selective proton transport, part 1: Wires preparation, Polymer (Guildf). 92 (2016) 50–57, https://doi.org/10.1016/j.polymer.2016.03.073.
[45] A. Zare, B. Pascual-Jose, S. de la Flor, A. Ribes-Greus, X. Montané, J.A. Reina, M. Giamberini, Membranes for cation transport based on dendronized poly (Epichlorohydrin-co-ethylene oxide). part 1: The effect of dendron amount and column orientation on copolymer mobility, Polymers (Basel) 13 (2021) 3532, https://doi.org/10.3390/polym13203532.
[46] T.B. Kohlan, A.E. Atespare, M. Yildiz, Y.Z. Menceloglu, S. Unal, B. Dizman, Synthesis and Structure-Property Relationship of Amphiphilic Poly(2-ethyl- co-2-(alkyl/aryl)-2-oxazoline) Copolymers, ACS Omega. 7 (2022) 40067–40077, https://doi.org/10.1021/acsomega.2c04809.
[47] M.E. Kourti, E. Fega, M. Pitsikalis, Block copolymers based on 2-methyl- and 2-phenyl-oxazoline by metallocene-mediated cationic ring-opening polymerization: Synthesis and characterization, Polym. Chem. 7 (2016) 2821–2835, https://doi.org/10.1039/c6py00405a.